

SUPPLEMENTARY INFORMATION

In situ Study of the Growth of Two-Dimensional Palladium Dendritic Nanostructures Using Liquid-Cell Electron Microscopy

Guomin Zhu^a, Yingying Jiang^a, Fang Lin^b, Hui Zhang^{a,*}, Chuanhong Jin^{a,*}, Jun Yuan^{a,c}, Deren Yang^a, Ze Zhang^a

^a State Key Laboratory of Silicon Materials, Key Laboratory of Advanced Materials and Applications for Batteries of Zhejiang Province, Department of Materials Science and Engineering, Zhejiang University, Hangzhou, Zhejiang 310027, P. R. China

^b College of Science, South China Agricultural University, Guangzhou, Guangdong 510642, P. R. China

^c Department of Physics, University of York, Heslington, York, YO10 5DD, United Kingdom

List of contents

Movie S1 shows the growth of palladium dendritic nanostructures (with nuclei precisely deposited by focused electron beam)

Movie S2 shows the growth of palladium dendritic nanostructures (with nuclei randomly formed)

Movie S3 shows the growth of palladium dendritic nanostructures starting from the left.

Movie S4 shows the growth of palladium dendritic nanostructures in the thick liquid layer, which can be taken as a 3D dendritic growth

Figure S1 shows the another example for the *in situ* growth of palladium 2D DNSs and the similar analysis as done for the case shown in the maintext (images from Movie S3)

Figure S2 shows the atomic force image of a DNS

Figure S3 gives the SAED pattern of the palladium DNSs shown in the maintext

Figure S4 HAADF image of edge of a palladium DNS

Figure S5 HRTEM image showing the edge structure of a palladium DNS

Figure S6 shows the formation of 3D palladium DNSs in thick liquid layers

Table S1 summarizes the growth rates of different metallic dendritic nanostructures in a few previous reports

Experimental Section

Stock solutions of tetrachloropalladate (99%, Aldrich) and potassium bromide (99.99%, Aladdin) were prepared by dissolving the salt in deionized water (Millipore grade) at a concentration of 0.9 mM and 90 mM respectively. All the chemicals were used as received without further purification. A liquid-fluid holder from Hummingbird Inc. USA was used for our experiments. Liquid was sealed by sandwiching two silicon microchips, and each of them is decorated with a SiN membrane (typically 50 nm thick) which is transparent to the incident high-energy electron beam in the microscope. Prior to liquid loading, SiN windows were cleaned with oxygen plasma for 5 minutes in order to remove organic contamination and render the surfaces hydrophilic. For the liquid loading, firstly a space chip (typically 500 nm thick about the space) was placed into the chip pocket on the holder, 1 μ L of aqueous solution was then deposited onto the chip with a pipette, a blank chip was finally placed on top of the first chip. A leakage detector based on a turbo-pumping system was used to assure the sealing. The microscope was well-aligned before any *in situ* liquid-cell experiments in order to decrease the side-effects of electron beam during the extra illuminations.

All the in situ experiments were carried out using a FEI Tecnai G² F20 microscope. The microscope was operated at 200 kV, acquiring 512×512 pixel images with a 3.16 μs dwell time for each pixel, using an average beam current of 500 pA. The probe size is estimated to ca. 0.53nm based on the equation: $d_p = (d_g + d_s + d_d)^{1/2}$ where d_g is the initial Gaussian diameter, d_s is the spherical aberration limited diameter, and d_d is the diffraction-limited diameter.[s1] CamStudio was used to capture screens and record all the movies showing the dynamic process. Radius and fractal dimension of DNSs were analyzed using the Image-J developed at the National Institutes of Health. Ex situ TEM and STEM characterizations were performed using a Tecnai G² F20 and a FEI ChemiSTEM operated at 200 kV.

Fractal dimension calculations:

We used the box dimension method to calculate the fractal dimension of the Pd dendritic structure. [s2] Boxes with the length of ϵ were used to cover the fractal. Count the number of occupied boxes, which was represented as $N(\epsilon)$. With the decrease of the length ϵ , $N(\epsilon)$ increased. $N(\epsilon)$ - ϵ curve was linear in logarithmic relationship, and the slope of the fitted line was the fractal dimension.

ImageJ with a plugin “FractalCount” was used to calculate the fractal dimensions. The fractal dimension did not vary obviously if we changed the threshold of the binary image, demonstrating the good reliability of our analysis.

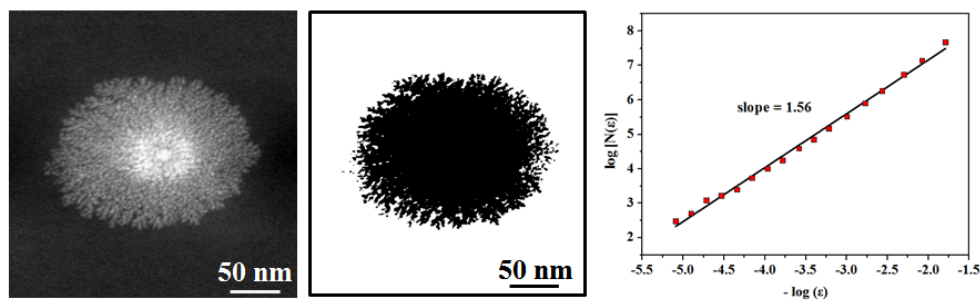


Illustration showing the workflow to calculate the fractal dimension.

Supplementary figures:

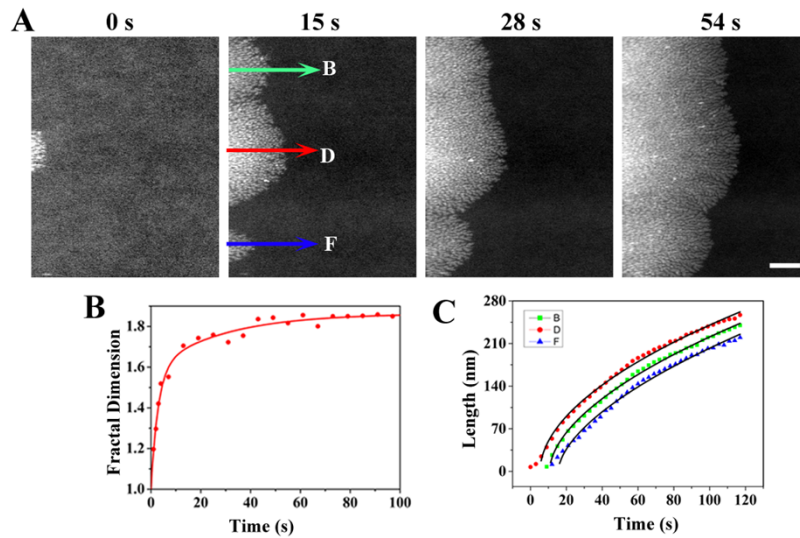


Figure S1. (A) Time lapse series following the growth of dendritic palladium nanostructures. The scale bar is 50 nm. (B) Fractal dimension of the dendritic nanostructures versus time. (C) Dendritic length (corresponding to that indicated in (A), with the same type of color) versus time. The black solid line is the result of a power law fit of the form $\langle l \rangle = K(t+b)^\beta$. The corresponding three cases: $\beta_F = 0.59 \pm 0.02$, $\beta_D = 0.55 \pm 0.02$, $\beta_B = 0.54 \pm 0.01$.

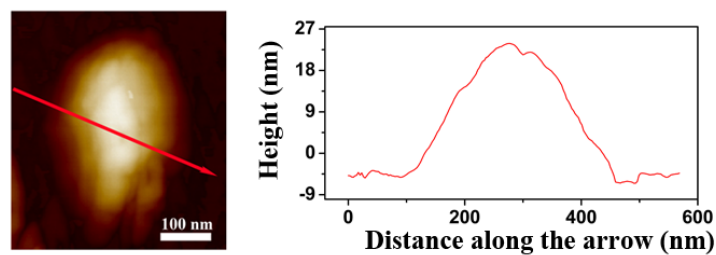


Figure S2. Atomic force image of a dendritic structure. The height in the center part is around 30nm.

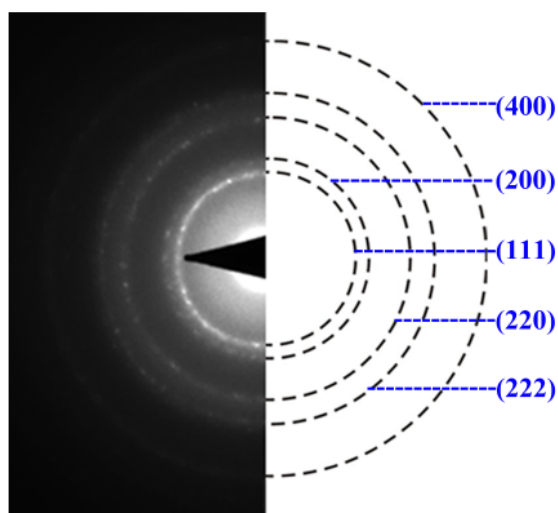


Figure S3. Selected area electron diffraction (SAED) pattern of the palladium DNSs confirming the polycrystalline feature

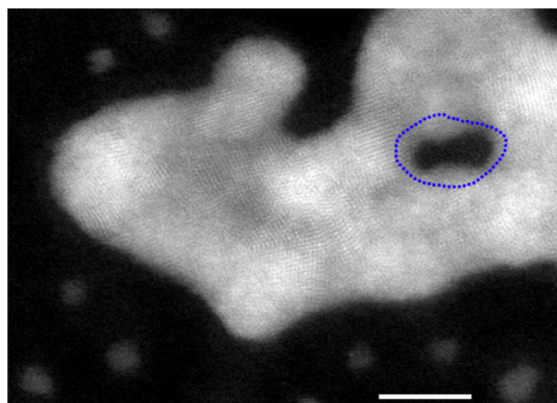


Figure S4. HAADF image of edge of a palladium DNS. Blue dotted circle indicates the void. Scale bar = 5 nm

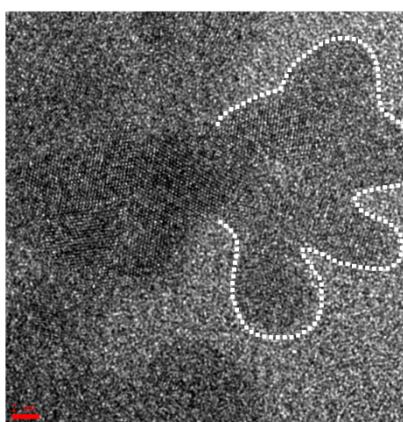


Figure S5. HRTEM image showing the edge structure of a palladium DNS. The dotted line in white draws out the morphology.

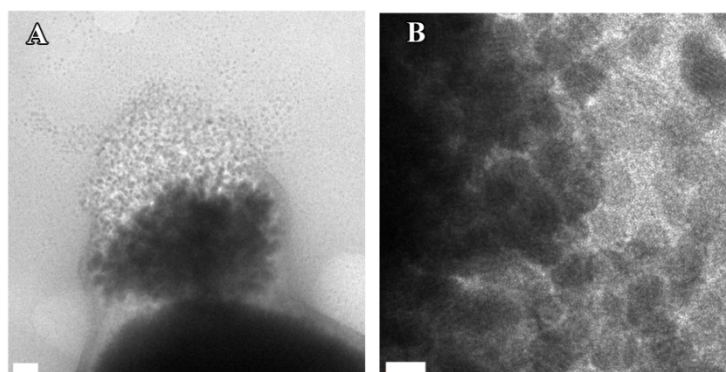


Figure S6. *Ex-situ* TEM images of dendritic nanostructures formed in thick liquid layer (movie S4). (A) Low magnification image of the dendritic nanostructures, scale bar = 20 nm. (B) High magnification image of the dendritic nanostructure, scale bar = 5 nm.

Table S1. Comparison of the growth rates reported in present experiments and the previous reported under conventional synthetic conditions

Product	Reaction time	Product size	Precursor concentration
2-D dendritic gold [s3]	~30 min	~1 μm	0.3 mM(HAuCl_4)
Branched palladium [s4]	160 min	~100 nm	10 mM(bis(acetonitrile) palladium dichloride)
Dendritic platinum [s5]	10 min	~20 nm	10 mM(K_2PtCl_4)
Dendritic copper [s6]	10 min	~5 μm	0.1 M (CuCl_2)
2-D dendritic palladium nanostructures in our case	~1 min	~300 nm	0.9 mM(Na_2PdCl_4)

Reference:

- S1 D. B. Williams, C. B. Carter. *Transmission electron microscopy*. Springer US, 2009. 83-84.
- S2. B. Chopard, J. Herrmann, T. Vicsek, *Nature*, 1991, **353**,409.
- S3. M. Pan, H. Sun, J. W. Lim, S. R. Bakaul, Y. Zeng, S. Xing, T. Wu, Q. Yan, H. Chen, *Chem. Commun.* 2012, **48**, 1440.
- S4. J. Watt, S. Cheong, M. F. Toney, B. Ingham, J. Cookson, P. T. Bishop, R. D. Tilley, *ACS Nano* 2010, **4**, 396.
- S5. L. Wang, Y. Yamauchi, *J. Am. Chem. Soc.* 2009, **131**, 9152.
- S6. R. Qiu, H. G. Cha, H. B. Noh, Y. B. Shim, X. L. Zhang, R. Qiao, D. Zhang, Y. I. Kim, U. Pal, Y. S. Kang, *J. Phys. Chem. C* 2009, **113**, 15891.